Corrosion inhibition by naturally occurring *Hibiscus sabdariffa* plant extract on a mild steel alloy in HCl solution

Magda Abdo Mahmoud AMEER*, **Amany Mohamed FEKRY**
Chemistry Department, Faculty of Science, Cairo University, Giza, Egypt

Abstract: The corrosion inhibition of mild steel alloys is of tremendous technological importance due to their increased industrial applications. Potentiodynamic polarization and electrochemical impedance spectroscopy techniques were used to establish the effect of different concentrations of HCl on the corrosion behavior of mild steel. A study was conducted on the inhibition of dissolution for a mild steel alloy in the most corrosive concentration of HCl (5 M) by adding different concentrations of aqueous extract of *Hibiscus sabdariffa* plant (named karkade or rosselle) as an ecofriendly inhibitor. The extent of corrosion inhibition as measured by the two techniques was comparable. The results indicated that the additive acts by way of adsorption as an effective protective inhibitor in aggressive acid medium. Curves representing the variation in the extent of adsorption or surface coverage as a function of the concentration of the additive are invariably sigmoid in nature. Generally the inhibition efficiency increases with increasing additive concentration.

Key words: Mild steel, corrosion, HCl, inhibitor, *Hibiscus sabdariffa*

1. Introduction

Acid solutions are often used in industry for cleaning and pickling of steel structures, processes that are normally accompanied by considerable dissolution of the metal. A useful method to protect metals and alloys in aggressive environments against corrosion is addition of species to the solution in contact with the surface in order to inhibit the corrosion reaction and reduce the corrosion rate.[1] Corrosion behavior of steels has received a considerable amount of attention as a result of its industrial importance. Corrosion inhibitors are widely used in industry to reduce the corrosion rate of different metals and alloys that are present in contact with aggressive environments. Many studies have been carried out to find suitable compounds to use as corrosion inhibitors. Use of inhibitors is one of the most practical methods for protection against corrosion, especially in acid solutions, to prevent unexpected metal dissolution and acid consumption.[2] Most of these compounds are synthetic chemicals that may be very expensive and hazardous to living creatures and environments. It is very important to choose cheap and safe to handle compounds for use as corrosion inhibitors. These natural organic compounds are either synthesized or extracted from aromatic herbs, spices, and medicinal plants. Plant extracts are viewed as an incredibly rich source of naturally synthesized chemical compounds that can be extracted by simple procedures low in cost and are biodegradable in nature. The use of these natural products such as extracted compounds from leaves or seeds as corrosion inhibitors has been widely reported by several authors.[3−8] Hibiscus tea is the infusion made from the calyces (sepals) of the *Hibiscus sabdariffa* flower. Hibiscus tea has a tart, cranberry-like flavor and contains vitamin C and minerals and is used traditionally as a mild medicine.[9] Therefore, in this study

*Correspondence: mameer_eg@yahoo.com

Hibiscus subdariffa plant extract was used as a natural product inhibitor due to the high antioxidant properties of the flowers calyxes, which have been extensively evaluated. [10] Karkade is the dry calyx and epicalyx of the flowers of *Hibiscus sabdariffa*. The two main constituents of the aqueous extracts of *Hibiscus sabdariffa* (roselle or karkade), namely the organic acids and the coloring materials, were effective in retarding the dissolution of the tested alloy. The activity of the coloring portion was considerably higher than that of the organic acids. [11]

The plants are rich in anthocyanins, as well as protocatechuic acid. The dried calyces contain the flavonoids gossypetin, hibiscetine, and sabdaretine. The major pigment, formerly reported as hibiscin, has been identified as daphniphylline. Small amounts of myrtillin (delphinidin 3-monoglucoside), chrysanthenin (cyanidin 3-monoglucoside), and delphinidin are also present. Roselle seeds are a good source of lipid-soluble antioxidants, particularly gamma-tocopherol. [9]

The aim of this work was to study the electrochemical corrosion rate on mild steel in different concentrations of hydrochloric acid solution. Corrosion inhibition of the most corrosive acid concentration was studied using *Hibiscus sabdariffa* plant as a natural product with different concentrations. Electrochemical techniques used were potentiodynamic polarization and impedance spectroscopy (EIS).

2. Results and discussion

2.1. EIS measurements

2.1.1. Effect of acid concentration

Figures 1a and 1b show the Bode and Nyquist plots for mild steel alloy in acid medium with different concentrations (0.5–5.0 M HCl), respectively. The experiments were performed after the working electrode was left in the test solution for 2 h reaching steady state potential value at 298 K. As shown in Figure 1a, increasing acid concentration leads to a decrease in the impedance value and the phase angle maximum, due to increasing aggressiveness of the medium. Moreover, the diameter of Nyquist plots (Figure 1b) decreases with increasing acid concentration, indicating a decrease in resistance. Computer simulation of the EIS results was performed using a complex nonlinear least-square (CNLS) fitting procedure in order to establish which electrical equivalent circuit (EEC) best fits the experimental data. The experimental impedance diagrams were fitted to the appropriate equivalent models shown as an inset in Figure 1b to analyze the cases with one time constant. In all cases, good agreement between theory and experiment was obtained for the whole frequency range with an average error of 5%. All curves show one time constant. Using a constant phase element (CPE), [12] the simple Randle's equivalent circuit was found to be satisfactory for fitting the impedance data. The model (Figure 1b) consisted of a solution resistance (R_s) in series with RC parallel combination (R/Q), which represents the charge transfer resistance and a constant phase element (Q) instead of an ideal capacitance element for the double layer, respectively, representing the corrosion product layer on the sample surface. [12] In this model the total cell impedance $Z(\omega)$ is represented by the following complex function: [12,13]

$$Z(\omega) = R_S + \frac{R}{1 + (j\omega)^\alpha RQ},$$ (1)

where ω is the angular frequency ($\omega = 2\pi f$ in rad s^{-1}) and $j^2 = -1$. In the case that the electrode surface is covered with a corrosion product layer, R and Q will be the resistance and capacitance of the layer, respectively. Since electrochemical systems show inhomogeneities and roughness of the surface, [14] the dispersive behavior is better described by means of a constant phase element (CPE). The impedance associated with the capacitances of the layers is described by the complex frequency dependent impedance (Z_{CPE}) defined as [12]
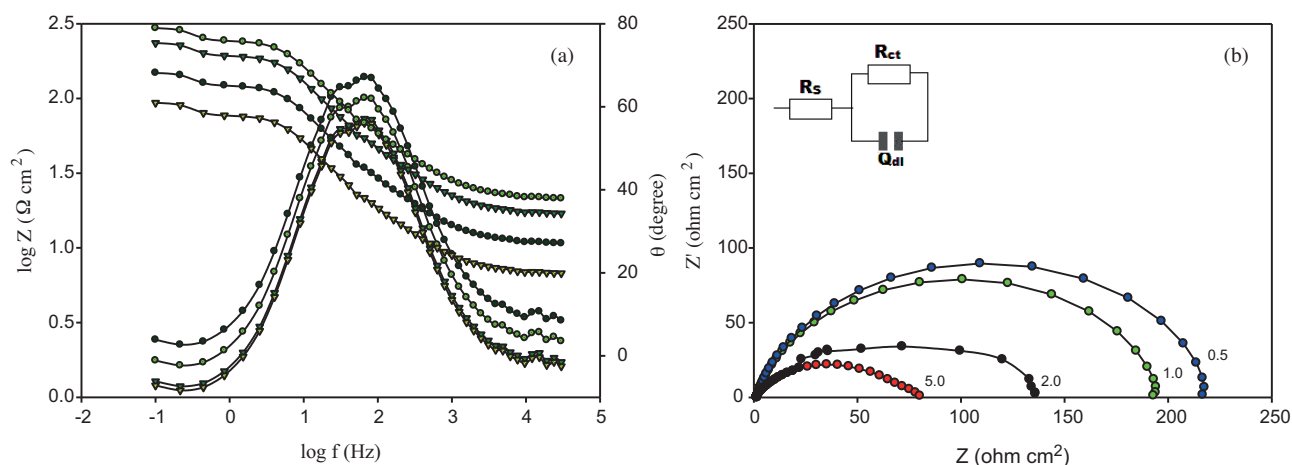
Figure 1. a) Bode and b) Nyquist plots of mild steel immersed for 2 h in different concentrations of HCl at 298 K, inserted in (b) an equivalent circuit that fits one time constant data.

$$Z_{CPE} = \frac{1}{(j\omega)^\alpha} \tag{2}$$

Values of α are the correlation coefficients for the CPE $(0 < \alpha < 1)$. The impedance parameters obtained are given in Table 1. Analysis of the experimental spectra was conducted using Thales software provided with the workstation where the dispersion formula suitable for each model was used.[12] In all cases, good conformations between theoretical and experimental results were obtained for the whole frequency range. Fitting parameters, given in Table 1, show that Q_{dl} value increases with increasing acid concentration, indicating that the corrosion product layer on the sample surface decreases with increasing acid concentration. This was confirmed by decreasing charge transfer resistance (R_{ct}) with increasing acid concentration.

Table 1. EIS fitted parameters for mild steel electrode immersed in different acid concentrations for 2 h at 298 K.

Conc. (mol/L)	R_s (Ω cm^2)	R_{ct} (Ω cm^2)	Q_{dl} (μF/cm^2)	α
0.5	12.5	223.5	24.5	0.89
1.0	5.20	194.5	36.3	0.88
2.0	4.10	141.3	39.1	0.88
3.0	4.00	100.5	47.3	0.86
5.0	3.80	89.40	50.1	0.87

2.1.2. Effect of inhibitor concentration

Karkade was added in different amounts to the most corrosive acid concentration (5 M HCl) as shown in Figures 2a and 2b for Bode and Nyquist plots, respectively. Impedance parameters given in Table 2 were evaluated after fitting using the model shown in Figure 2b. It was found that the charge transfer resistance of the steel surface layer increases with increasing karkade concentration until 40 mg/L, which is due to increasing adsorption activity of organic acids and coloring materials that retard alloy dissolution.[11] Figure 2 reveals generally concurrent features to the behavior of the layer resistance, where it increases with increasing inhibitor concentration. The increase in the corrosion rate can be rationalized on the basis that the acid reacts with iron and forms metal chloride, which is soluble in aqueous media. Two reactions occur: the anodic reaction and cathodic reaction. The following equations represent the iron reaction in acidic solutions:[13]
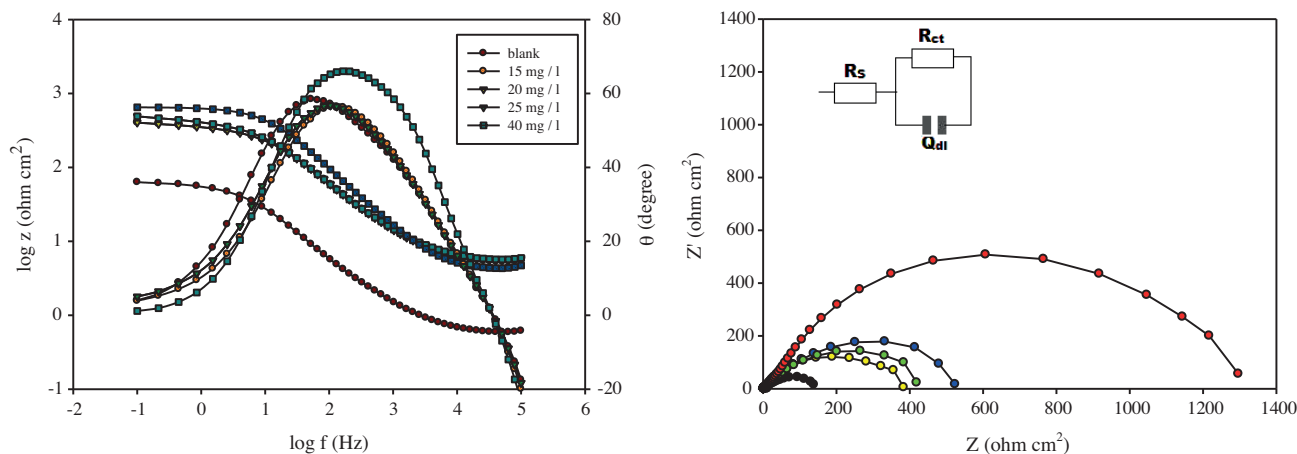
Figure 2. a) Bode and b) Nyquist plots of mild steel immersed for 2 h in different concentrations of karkade extract in 5 M HCl at 298 K, inserted in (b) an equivalent circuit that fits one time constant data.

Table 2. EIS fitted parameters and inhibition efficiency for mild steel electrode in 5.0 M HCl in the absence and presence of different concentrations of karkade extract at 298 K.

C (mg/L)	R_s (Ω cm^2)	R_{ct} (Ω cm^2)	Q_{dl} (μF/cm^2)	α	IE%
0.00	3.80	79.40	50.1	0.87	0.00
15	2.10	457.1	30.3	0.91	82.6
20	2.30	501.2	21.6	0.93	84.2
25	2.50	561.3	19.5	0.95	84.5
40	2.90	1258.9	15.4	0.96	93.7

Anodic reaction (oxidation reaction):

$$Fe \rightarrow Fe^{2+} + 2e \tag{3}$$

Cathodic (reduction reaction or hydrogen evolution reaction):

$$2H^+ + 2e \rightarrow H_2 \uparrow \tag{4}$$

Inhibition efficiency at different karkade concentrations was calculated and tabulated in Table 2 using the following equation:

$$\%IE = \frac{R_{(inhibited)} - R^o_{(Blank)}}{R_{(inhibited)}}, \tag{5}$$

where R° and R are the resistances for steel in the absence and presence of inhibitors, respectively.

It was found that the inhibition efficiency increases with increasing inhibitor concentration, reaching 93.7%. This might be due to the adsorption of inhibitor molecule on the metal surface as a protective layer giving high inhibition efficiency. Moreover, karkade contains large amounts of mucilage, which is gelatinous or slimy polysaccharides that increase its adsorption on the metal surface.[9]

2.1.3. Effect of immersion time

The stability of the layer formed on the mild steel alloy after immersion in 5 M HCl containing 40 mg/L karkade for 480 h at 298 K was studied as shown in Figures 3 and 4 as Bode and Nyquist plots, respectively. As shown in Figure 3a and Figure 4a, the appearance of a shoulder on the phase angle curves at lower frequencies, which shifts the curves into two different frequency regions, is the response of at least two different frequency-dependent processes with two corresponding time constants. The experimental impedance diagrams were fitted to the appropriate equivalent models shown as an inset in Figure 5 to analyze the cases with two time constants. In all cases, good agreement between theory and experiment was obtained for the whole frequency range with an average error of 5%. The estimated theoretical impedance parameters are collected in Table 3 for a mild steel electrode immersed in 5.0 M HCl containing 40 mg/L karkade extract with immersion time at 298 K. The five element RQ equivalent circuit with two lumped time constants is necessary for modeling faradaic processes involving the adsorption of two different species as shown in Figure 5. This circuit has several structures; one of them is the Voight model, where its impedance expression is as follows:[15]

$$Z(\omega) = R_S + \frac{R_1}{1 + R_1 Q_1 (j\omega)^{\alpha_1}} + \frac{R_2}{1 + R_2 Q_2 (j\omega)^{\alpha_2}} \tag{6}$$
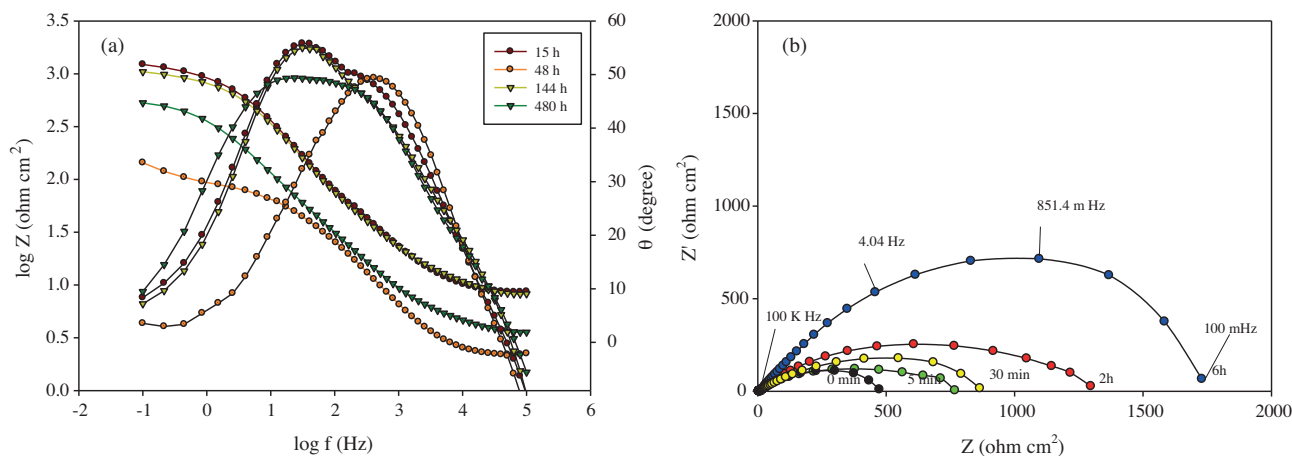
with $0 \leq \alpha_1, \alpha_2 \leq 1$
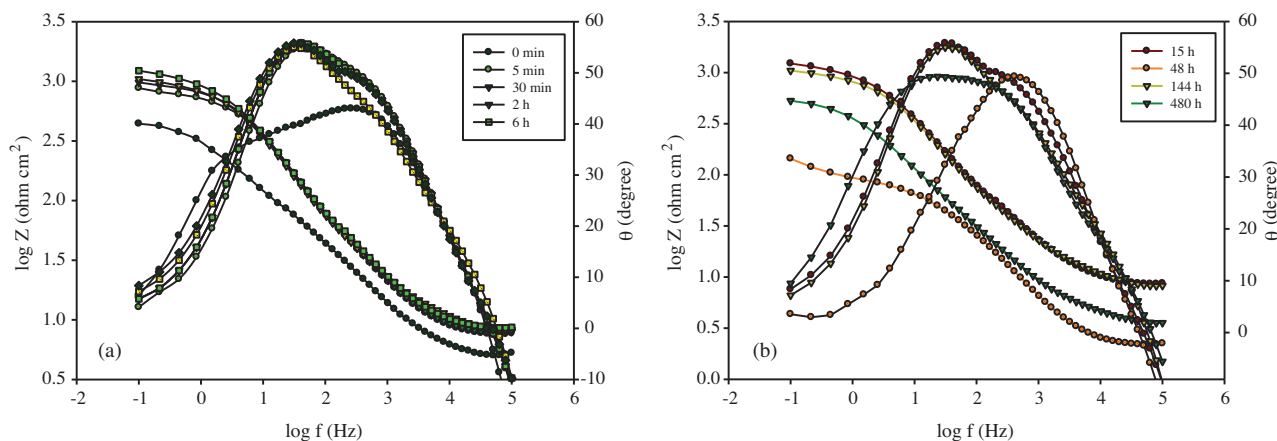
Figure 3. Bode plots of mild steel in 5 M HCl containing 40 mg/L karkade extract at 298 K, with immersion time from a) 0–6 h and b) 15–480 h.

Table 3. EIS fitted parameters for mild steel electrode immersed in 5.0 M HCl containing 40 mg/L karkade extract with immersion time at 298 K.

α_2	Q_2 ($\mu F/cm^2$)	$R_2/$ (Ω cm^2)	α_1	Q_1 ($\mu F/cm^2$)	R_1 (Ω cm^2)	R_s (Ω cm^2)	Time (h)
0.93	23.1	430.9	0.78	70.3	70.1	3.2	0.00
0.95	22.5	757.5	0.76	61.1	92.3	3.0	0.50
0.97	13.2	1305.4	0.87	51.4	279.6	3.0	6.00
0.96	14.7	1282.3	0.88	47.1	107.5	3.9	15.00
0.97	12.8	1464.9	0.86	35.8	315.1	4.1	48.00
0.96	17.1	1077.9	0.79	43.9	182.2	5.2	144.00
0.98	22.7	271.7	0.76	66.7	126.3	2.0	480.00

Figure 4. Nyquist plots of mild steel in 5 M HCl containing 40 mg/L karkade extract at 298 K, with immersion time of a) 0–6 h and b) 15–480 h.
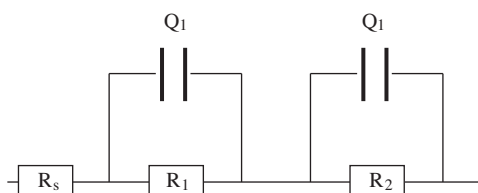
Figure 5. Equivalent circuit model representing two time constants for an electrode/electrolyte solution interface.

Fitting procedures have shown that good agreement between the theoretical and experimental data is obtained if a frequency-dependent constant phase element is introduced instead of a pure capacitor. This EEC consists of two circuits in series from $R_1 Q_1$ and $R_2 Q_2$ parallel combination and the two are in series with the solution resistance (R_S). In this way Q_1 is related to combinations from the capacitance of the outer layer and Q_2 of the inner layer, while R_1 is the resistance of the sealed pores by the corrosion products in the outer layer and R_2 of the inner layer.[15] The simulated response of the representative circuit compares well with the experimental results in both admittance and impedance planes. This indicates that the suggested model is suitable for explaining the behavior of mild steel in 5 M HCl containing 40 mg/L karkade at different time intervals. The equivalent circuit parameters are presented in Table 3. It was found that the layer is stable up to 48 h with an increasing impedance value ($R_T = R_1 + R_2$) as shown in Figure 6 and the diameter of Nyquist plots also increases. This is due to the extent of adsorption increases with increasing immersion time shielding the reactive metal surface from the aggressive acid medium,[16,17] leading to a decrease in corrosion rate. After 48 h of immersion until 480 h $\approx$ 20 day, the corrosion rate increases, which may be due to the dissolution of organic acids in karkade in aggressive 5 M HCl medium.

## 2.2. Potentiodynamic polarization measurements

2.2.1. Effect of acid concentration

The potential was scanned automatically from –1.2 to –0.4 V vs. SHE at a rate of 1 mV s^{-1}, which allows quasistationary state measurements. Prior to the potential scan the electrode was left under open circuit conditions in the respective solution for 2 h until a steady free corrosion potential value was recorded. These

results enable the determination of various electrochemical corrosion parameters of the two electrodes using Thales software for i/E analysis.[12] To avoid the presence of some degree of nonlinearity in the Tafel region of the obtained polarization curves, the Tafel constants were calculated as the slope of the points after E_{corr} by 50 mV, using computer least squares analysis. The corrosion current was then determined by the intersection of the cathodic or the anodic Tafel line with the potential of zero current in the potentiodynamic curves or E_{corr}. This point determines the potential (E_{corr}) and current density (j_{corr}) for corrosion. For all tested electrodes the active dissolution parameter values, corrosion potential (E_{corr}), corrosion current density (j_{corr}), and Tafel slopes (β_a and β_c) were calculated and are presented in Table 4. Figure 7 shows polarization curves for the steel in different HCl concentrations. It is clear that i_{corr} value increases with increasing HCl concentration, indicating an increase in the corrosion rate of the surface. It is also noted that the corrosion potential shifts towards more negative potential as acid concentration increases. Figure 8 shows a decrease in the logarithm of corrosion current density with increasing acid concentration logarithm, giving a linear relation. This is confirmed by increasing i_{corr} value as given in Table 4. This confirms that the corrosion rate increases with increasing aggressiveness of the medium (acid concentration).

Table 4. Electrochemical parameters for a mild steel electrode immersed in different acid concentrations for 2 h at 298 K.

Conc. (mol/L)	$-E_{corr}$ (mV)	i_{corr} (μA/cm^2)	$-\beta_c$ (mV/dec)	β_a (mV/dec)
0.5	524.1	294.5	152	84
1.0	542.2	420.3	117	81
2.0	545.9	586.1	213	127
3.0	560.1	609.5	215	130
5.0	570.8	745.8	212	133
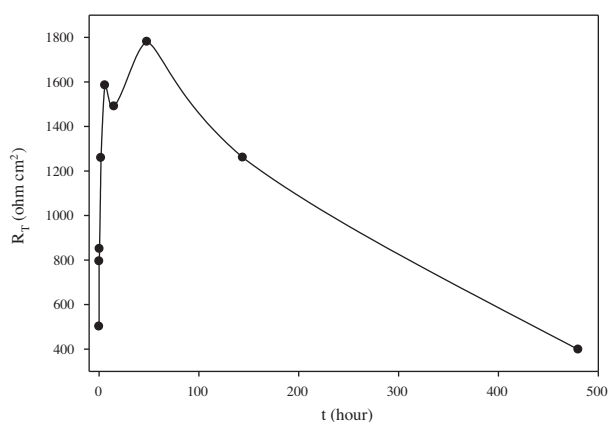
Figure 6. Effect of immersion time on R_T for mild steel in 5 M HCl containing 40 mg/L karkade extract at 298 K.
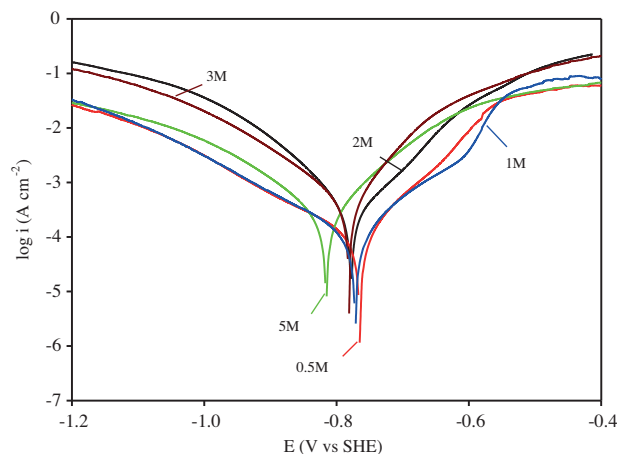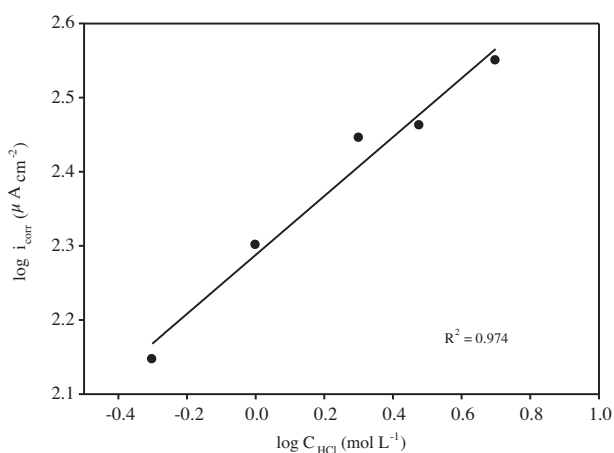

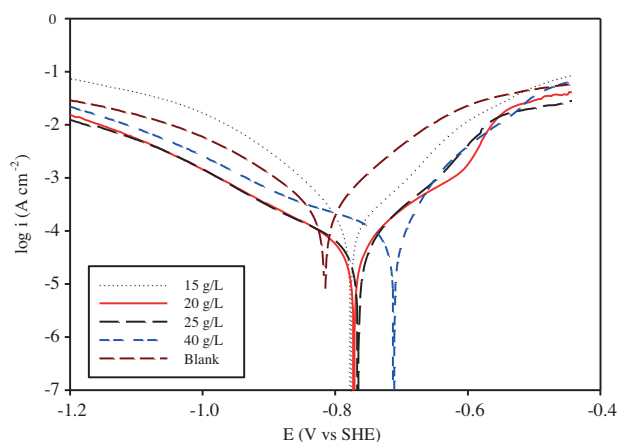**Figure 7.** Polarization scans of mild steel immersed for 2 h in different concentrations of HCl at 298 K.

2.2.2. Effect of inhibitor concentration

Figure 9 shows potentiodynamic scans after addition of karkade in different amounts per liter as inhibitor in 5 M HCl. The potential was also scanned from –1.2 to –0.4 V vs. SHE at a rate of 1 mV s^{-1} after immersion of the electrode in the respective solution for 2 h. The scans show that corrosion current density decreases

with increasing inhibitor concentration, indicating a decrease in the corrosion rate. This can be attributed to deposition of the inhibitor molecules on the alloy as a result of interaction between the inhibitor and the metal surface that can effectively seal the surface against further reaction. Karkade consists of 3.5% proteins, 10% liquids, 63.5% glucides, 11% cellulose, and 12% ash (Fe, Mn, Al, Na, K, SO_4, PO_4, and Cl). The glucides are 22% organic acids and 16% reducing sugars and 25% other nonnitrogenous substances. The water soluble acids consist of 77% citric acid, 22% malic acid, and traces of tartaric acid. The coloring matter contained in flowers of *Hibiscus subdariffa* is a mixture of hibiscetin (3:5:7:8:3':4':5'-heptahydroxyflavone) and gossypetin (3:5:7:8:3':4'-hexahydroxyflavone). The glycosidic bond is at the 3-position. The dried drug contains also about 40–50 mg of ascorbic acid (vitamin C)/100 g.[10] In addition, the large amounts of mucilage in karkade, which is gelatinous or slimy polysaccharides, perhaps increase its adsorption on the metal surface.[9]

Figure 8. Variation in log i_{corr} value with log C_{HCl} of mild steel at 298 K.

Figure 9. Polarization scans of mild steel immersed for 2 h in different concentrations of karkade extract in 5 M HCl at 298 K.

The *Hibiscus sabdariffa* petals are potentially a good source of antioxidant agents as anthocyanins and ascorbic acid.[18]

The inhibition efficiency is given by the following equation:[17,18]

$$IE\% = 1 - \frac{i_{inh}}{i_{corr}} \times 100, \tag{7}$$

where i_{corr} and i_{inh} refer to the corrosion current densities in the absence and presence of inhibitor, respectively, and are determined by extrapolation of cathodic and anodic Tafel lines to corrosion potential. The electrochemical parameters are collected in Table 5. It is observed that the corrosion potentials E_{corr} shift to less negative values (noble direction) with increasing extract concentration. This indicates that the addition of *Hibiscus subdariffa* (karkade) extract primarily affects the anodic process, and acts predominately as an anodic-type inhibitor. Consequently, the adsorption of the extracts in HCl solutions is more likely at anodic sites. Furthermore, the values of the corrosion current density (i_{corr}) decreased with increasing concentration of the extracts, indicating an inhibitive property of these extracts on the corrosion of mild steel in acid solutions. Cathodic Tafel slope, β_c, and anodic Tafel slope, β_a, are more or less constant upon increasing the extract concentrations. These results indicate that the extracts act by simple blocking of the available cathodic and anodic sites on the mild steel surface. In the other words, these inhibitors decrease the surface area for corrosion

without affecting the mechanism of the corrosion process and only cause inactivation of a part of the metal surface with respect to corrosive medium. Moreover, the inhibition efficiency, IE%, for extracts increases with increasing concentration, and at higher inhibitor concentration (40 mg/L), IE% reaches 91.4%, as shown in Figure 10.

Table 5. Electrochemical parameters and inhibition efficiency for a mild steel electrode in 5.0 M HCl in the absence and presence of different concentrations of karkade extract at 298 K.

C (mg/L)	$-E_{corr}$ (mV)	i_{corr} (μA/cm^2)	$-\beta_c$ (mV/dec)	β_a (mV/dec)	IE%
0.00	570.8	745.8	212	133	0.00
15	520.2	109.8	194	49.2	85.3
20	480.8	97.5	197	50.5	86.9
25	460.7	79.2	202	52.6	89.3
40	455.1	64.5	210	55.3	91.4

The relation between C/θ (C is the inhibitor concentration and θ is the surface coverage of the adsorbed layer; θ = IE/100 from both EIS and Tafel) and C at 25 °C in 5 M HCl with various concentrations of *Hibiscus subdariffa* (Karkade) extracts is shown in Figure 11. It reveals that a straight line was obtained with slope close to unity, indicating that the adsorption of plant extracts obeys the Langmuir adsorption isotherm.[19−21] This involves the assumption of no interaction between the adsorbed inhibitor constituents on the steel surface. The Langmuir isotherm is based on the assumption that each site of the metal surface holds one adsorbed species. Therefore, one adsorbed H_2O molecule is replaced by one molecule of the inhibitor adsorbate (plant extracts) on the steel surface.
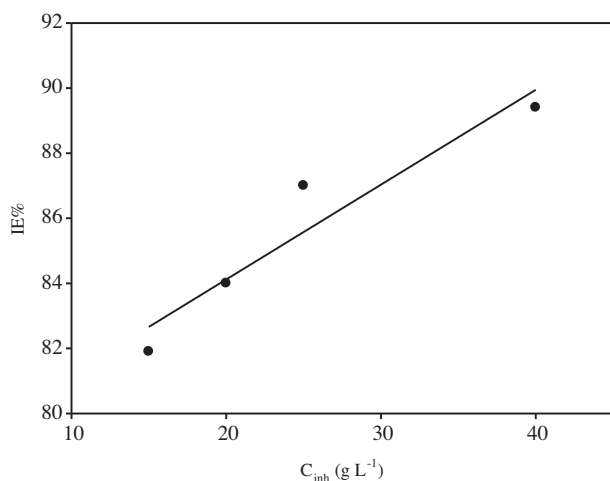
Figure 10. S-shape diagram of the variation in inhibition efficiency with karkade extract concentration.
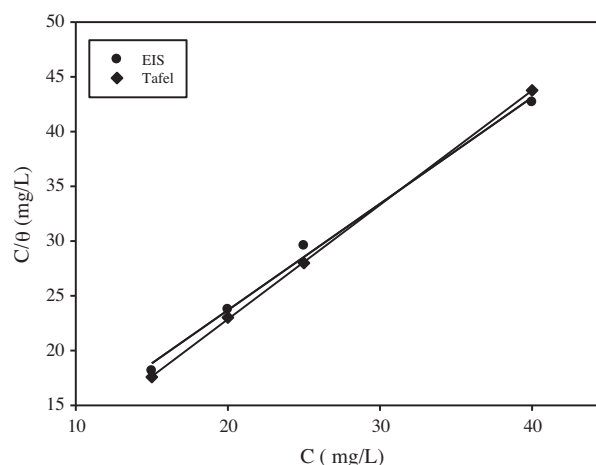
Figure 11. Variation in C/θ with karkade extract concentration (Langmuir isotherm).

With regard to the Langmuir adsorption isotherm according to the following equation:

$$C/\theta = (1/K_{ads}) + C \tag{8}$$

K_{ads} is the adsorption–desorption equilibrium constant. By plotting C/θ versus C at 298 K, a straight line is obtained as seen in Figure 11. The adsorption equilibrium constant, K_{ads}, is related to the standard free

energy, ΔG_{ads}°, with the following equation:

$$K = \frac{1}{C_{H_2O}} \exp\left(-\frac{\Delta G_{ads}^{\circ}}{RT}\right), \tag{9}$$

where C_{H_2O} is the concentration of water in solution expressed in mol/L, R is gas constant, and T absolute temperature. At 298 K, the average value of standard adsorption free energy ΔG_{ads}° was –30 kJ/mol. The negative value of ΔG_{ads}° ensures the spontaneity of the adsorption process and stability of the adsorbed layer on the metal surface.

The results showed that R_{ct} value increases with increasing inhibitor concentration, indicating a decrease in the corrosion rate of the steel. The corrosion rate (i_{corr}) increases with decreasing inhibitor concentration. EIS measurements under open circuit conditions confirmed the polarization results well. On adding 40 mg/L karkade concentration, it shows very good inhibition efficiency (IE) in 5 M HCl solution, reaching 93.7% as calculated from EIS measurements and 91.4% from polarization measurements. This means that the two techniques confirm each other.

3. Experimental

The steel rod used in this study had a cross-sectional area of 0.47 cm^2. The composition of the steel was as follows (wt %): C = 0.31, Si = 0.21, Mn = 0.81, P = 0.014, S = 0.017, Cu = 0.06, Cr = 0.02, Mo = 0.01, Ni = 0.02, Sn = 0.0, V = 0.002 and the balance was Fe. The test solution was hydrochloric acid (Aldrich) of different concentrations (0.5, 1.0, 2, 3, and 5 M). Triple distilled water was used for preparing all solutions. In all measurements, the electrode was mechanically polished using successively finer grade emery papers (600–1200 grade). Polarization and electrochemical impedance spectroscopy (EIS) measurements were carried out using the electrochemical workstation IM6e Zahner-electrik GmbH, Meβ technik, Kronach, Germany. The excitation AC signal had an amplitude of 10 mV peak to peak in a frequency domain from 0.1 Hz to 100 kHz. The EIS was recorded after reading a steady-state potential. The scanning was carried out at a rate of 1 mV/s over the potential range from –1.2 to –0.4 V vs. a standard hydrogen electrode (SHE). Prior to the potential sweep, the electrode was left under open-circuit in the respective solution for 2 h until a steady-state corrosion potential was recorded. Corrosion current density, i_{corr}, which is equivalent to the corrosion rate, is given by the intersection of the Tafel lines' extrapolation. Because of the presence of a degree of nonlinearity in part of the obtained polarization curves, the corresponding Tafel slopes (β_a and β_c) and the corrosion current (i_{corr}) were calculated as a slope of the points after corrosion potential (E_{corr}) by ± 50 mV using computer least-square analysis. All potentials were measured with respect to SHE.

The fresh leaves of *Hibiscus sabdariffa* plant were washed under running water, shade dried, powdered into small pieces, and the powdered leaves were dissolved in triple distilled water and left overnight. Then the solution was filtered and stored. The concentrations of the extracts are expressed as mg/L (15, 20, 25, and 40).

References

1. Oguzie, E. *Corros. Sci.* **2008**, *50*, 2993–2998.
2. Sorkhabi, H.; Seifzadeh, D.; Hosseini, M. *Corros. Sci.* **2008**, *50*, 3363–3370.
3. Sorkhabi, H.; Asghari, E. *Electrochim. Acta.* **2008**, *54*, 162–167.

4. Gerengi, H.; Sahin, H. *Ind. Eng. Chem. Res.* **2012**, *51*, 780–787.

5. Okafor, P.; Ikpi, M.; Uwah, I.; Ebenso, E.; Ekpe, U.; Umoren, S. *Corros. Sci.* **2008**, *50*, 2310–2317.

6. Radojcic, I.; Berkovic, K.; Kovac, S.; Furac, J. *Corros. Sci.* **2008**, *50*, 1498–1504.

7. Ameer, M. *Mater. Chem. Phys.* **2010**, *122*, 321–324.

8. Yaro, A.; Khamom, A.; Wael, R. *Alexandria Engineering J.* **2013**, *55*, 129–135.

9. Fernandez, M.; Pineda, J.; Aguilar, M. *Food Sci.* **2007**, *72*, S207–S211.

10. Mendoza, J.; López, S.; Galindo, A.; Sandoval, J. *Food Eng.* **2008**, *87*, 391–397.

11. El Hosary, A.; Saleh, R.; Shams El Din, A. *Corros. Sci.* **1972**, *12*, 897–904.

12. Ghoneim, A.; Fekry, A.; Ameer, M. *Electrochim. Acta.* **2010**, *55*, 6028–6035.

13. Fekry, A.; Ameer, M. *Int. J. Hyd. Energ.* **2010**, *35*, 7641–7651.

14. Esplandiu, M.; Patrito, E.; Macagno, V. *Electrochim. Acta.* **1995**, *40*, 809–815.

15. Patrito, E.; Macagno, V. Electroanal. *Chem.* **1994**, *375*, 203–211.

16. Ergun, Ü.; Yüzer, D.; Emregül, K. *Mater. Chem. Phys.* **2008**, *109*, 492–499.

17. Fekry, A.; Mohamed, R. *Electrochim. Acta.* **2010**, *55*, 1933–1939.

18. Prenesti, E.; Berto, S.; Daniele, P.; Toso, S. *Food Chem.* **2007**, *100*, 433–438.

19. Ameer, M.; Fekry, A. *Int. J. Hyd. Energ.* **2010**, *35*, 11387–11396.

20. Ameer, M.; Fekry, A. *Progs. Org. Coat.* **2011**, *71*, 343–349.

21. Ameer, M.; Fekry, A.; Othman, A. *Int. J. Electrochem. Sci.* **2014**, *9*, 1964–1985.